ELSEVIER

Biochimica et Biophysica Acta 1477 (2000) 122–145

BIOCHIMICA ET BIOPHYSICA ACTA
BBA

www.elsevier.com/locate/bba

Review

Structure–function relationships of glutamine synthetases[1]

David Eisenberg *, Harindarpal S. Gill, Gaston M.U. Pfluegl, Sergio H. Rotstein

UCLA-DOE Laboratory of Structural Biology and Molecular Medicine, Departments of Chemistry, Biochemistry and Biological Chemistry, University of California, Los Angeles, 201 MBI, Box 951570, Los Angeles, CA 90095-1570, USA

Received 1 November 1999; accepted 1 December 1999

Abstract

As a highly regulated enzyme at the core of nitrogen metabolism, glutamine synthetase has been studied intensively. We review structural and functional studies of both bacterial and eukaryotic glutamine synthetases, with emphasis on enzymatic inhibitors.

Keywords: Glutamine synthetase; Kinetic study; Feedback inhibition; Structural study; Mechanism of action

1. Introduction

Professor Hans Neurath has devoted a lifetime to understanding proteolytic enzymes and inhibitors, but his interests are not contained within these bounds. His fascination with the fundamental ideas and methods of biochemistry led to his other career, as a great scientific editor, and account also for his broad interest in proteins in general.

Many scientists have contributed to our present knowledge of the enzymology of the glutamine synthetases, including the laboratories of Meister, Stadtman, Ginsburg, Wedler, Chock, Boyer, Kutsu and Magasanik. Very useful reviews include those of Ginsburg [1], Chock and Stadtman [2], Stadtman and Ginsburg [3], Wedler and Toms [4] and Purich [5]. Here we review from a structural perspective work on the activity and inhibition of glutamine synthetase, both in bacteria and higher organisms.

2. Overall structure of bacterial glutamine synthetase

The structure of GS was determined by X-ray crystallography initially to 3.5 Å resolution [6]. Subsequent rounds of data collection and refinement have extended the resolution to 2.5 Å [7–11]. The initial X-ray structural studies were on GS samples purified from a mutant *Salmonella typhimurium* strain, unable to adenylylate GS [12], to avoid heterogeneity from covalent modification. More recently, *S. typhimurium* GS has been expressed via recombinant methods using a glutamine auxotroph strain of *Escherichia coli*, YMC21 [13], which has been further modified for expression to yield either fully adenylylated GS [14] or fully non-adenylylated GS (J. Bowie, and D. Eisenberg, unpublished data). *S. typhimurium* GS has a molecular mass of 620 kDa. *Mycobacterium tuberculosis* GS (TB-GS) has a mo-

Abbreviations: GS, glutamine synthetase; TB-GS, glutamine synthetase from *Mycobacterium tuberculosis*; MetSox, methionine sulfoximine; PPT, phosphinothricin; MetSox ~ P[ADP], phosphorylated MetSox and ADP bound in an active site of GS

* Corresponding author. Fax: +1-310-206-3914;
E-mail: david@mbi.ucla.edu

[1] This review is dedicated to Professor Hans Neurath on his 90th birthday.

0167-4838/00/$ – see front matter
PII: S0167-4838(99)00270-8

lecular mass of 640 kDa. It has been expressed in the same *E. coli* recombinant system, crystals have been grown, and the structure is being determined to 2.4 Å resolution [15].

Bacterial GS molecules are dodecamers formed from two face-to-face hexameric rings of subunits, with 12 active sites formed between monomers [6,16]. Each active site can be described as a 'bifunnel' in which ATP and glutamate bind at opposite ends (Fig. 1). We refer to the ATP binding site as the top of the bifunnel, because it opens to the external 6-fold surface of GS. At the joint of the bifunnel are two divalent cation binding sites, n1 and n2, separated by 6 Å, where either magnesium or manganese bind for catalysis. The n2 ion is involved in phosphoryl transfer [17], while the n1 ion stabilizes an active GS [18] and plays a role in binding glutamate [19]. The affinity for metal ions at the n1 site is 50 times greater than at the n2 site [19]. This is caused by greater negative charge toward the bottom half of the bifunnel in the vicinity of n1 [11].

The GS dodecamer is held together mainly by hydrophobic and hydrogen bonding interactions between the two hexameric rings [6]. Both the N-terminus and C-terminus of each subunit are helical. The N-terminal helix sits above the hexameric ring and is exposed to solvent. The C-terminal helix, called the 'helical thong,' is inserted into a hydrophobic hole in the eclipsed subunit on the opposite hexameric ring. In Fig. 1, the helical thong is visible as the large rod-like structure extension from the bottom of the isolated subunit. In addition, the central channel of the dodecamer is lined by six four-stranded β-sheets, each built from an antiparallel loop (residues 137–152) contributed by subunits in opposite rings. One of these antiparallel loops is visible as a bent rod at the lower left of Fig. 1, to the right of the larger helical thong. The 12 thongs and six sheets give the dodecamer additional adhesion.

The structure of the dodecamer exposes several loops which are believed to have functional importance. One loop, which consists of hydrophilic residues 156–173, protrudes into the central channel of the dodecamer and is a site for proteolysis [20] and ADP-ribosylation [21]. Fig. 1 shows this loop forming crescent ridges in the central channel of the blue molecule and again as the far right ring-like structure on the isolated subunit. Another loop is the adenylylation loop, so called because it contains tyrosyl residue 397 which is covalently modified by addition of AMP [22]. This loop sits just outside the bottom entrance to the bifunnel. Other loops will be described in the following text and in [11].

3. GS-catalyzed reactions

GS is known to catalyze a variety of reactions summarized in a review by Stadtman and Ginsburg [3]. The catalytic activity of bacterial GS is regulated by two types of covalent modification: adenylylation [1], where the type of metal ion and pH play a role in GS activity, and by oxidative modification [23,24]. These regulatory mechanisms influence the following reactions.

3.1. Biosynthetic reaction

GS catalyzes glutamine biosynthesis via the reaction:

$$\text{Glutamate} + NH_4^+ + ATP \xrightarrow{Me^{2+}} \text{glutamine} + ADP + P_i + H^+ \quad (1)$$

where Me^{2+} can be magnesium or manganese. The reaction has been termed the 'biosynthetic' reaction and is considered the most physiologically relevant reaction that GS catalyzes. If hydroxylamine (NH_2OH) is substituted for the ammonium substrate in Reaction 1, the product glutamine is changed to γ-glutamylhydroxamate [25]. Either of these reactions is sometimes referred to as the 'forward' reaction and used in kinetic studies.

3.1.1. Two-step mechanism

From early studies, a two-step model for the mechanism of the biosynthetic reaction emerged [26–31]. The first step is the formation of the activated intermediate γ-glutamyl phosphate. The n2 ion coordinates the γ-phosphate oxygens of ATP to allow phosphoryl transfer to the γ-carboxylate group of glutamate, yielding the intermediate. This is followed by a second step – attack on the intermediate by ammonia – which releases free phosphate to yield glutamine.

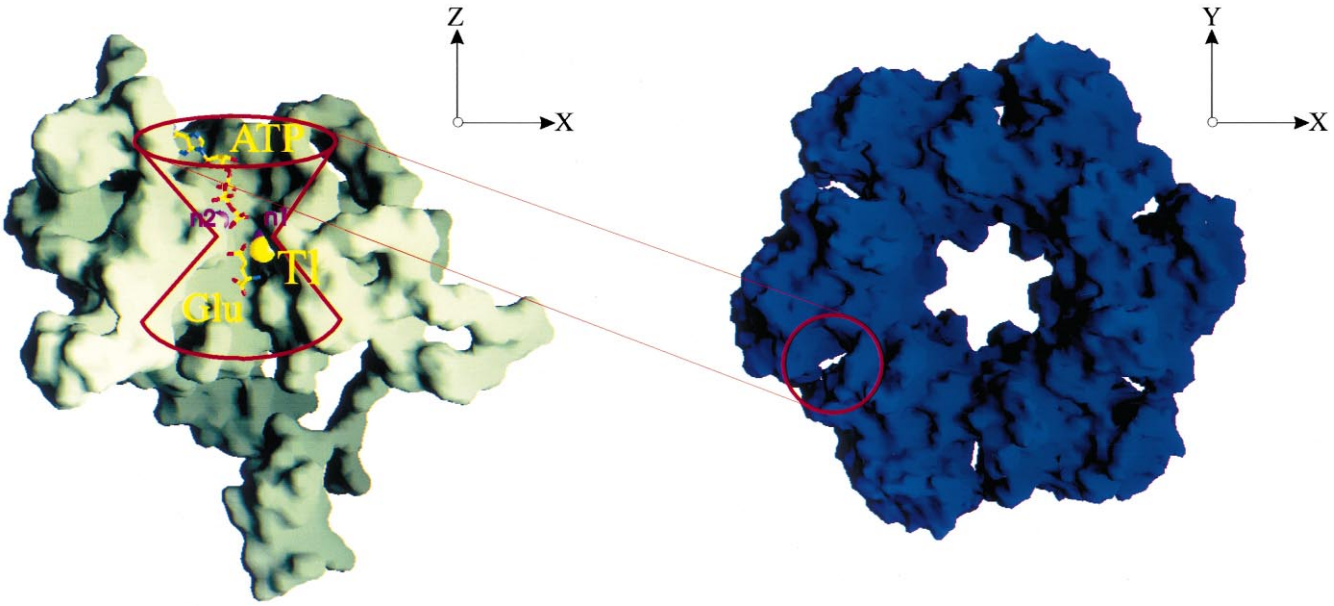

Fig. 1. Structure of bacterial glutamine synthetase. Bacterial glutamine synthetase is a dodecamer having 622 symmetry, with six two-fold axes perpendicular to a six-fold axis [6,15,31]. One of the two eclipsed hexameric rings is shown in blue. The dimensions of the dodecamer including the side chains are approximately 100 Å along the six-fold axis and 140 Å along a two-fold axis. The dodecamer has 12 active sites, one formed between every two neighboring subunits within a ring (shown by red circle). Each active site is a bifunnel, having entrances at the top and bottom for substrates ATP and glutamate, respectively. The green structure represents the C-terminal domain (residues 101–468) of one subunit. The molecular six-fold axis (*Z*) is shown to the right of the subunit. The bifunnel is about 30 Å wide at its opening, 15 Å wide at its middle, and 45 Å deep. The two metal ions (n1 and n2) are 6 Å apart, located at the neck of the bifunnel. The location of the ammonium substrate has been determined from its Tl^+ analog in Tl^+–GS complexes. The distance between the n1 and Tl^+ sites is 4 Å, and between n2 and Tl^+ is 7 Å [44]. To offer a clear view of the glutamate substrate, residues 326–328 of the Glu-327 flap have been removed. Notice the helical thong and β-loop extending from the bottom of the subunit, where they interact with the subunit below (see text).

Meister and coworkers inferred the two step mechanism. The formation of pyrrolidone carboxylate[2] (a cyclized product of γ-glutamyl phosphate) upon brief heating of a mixture of ATP, magnesium, L-glutamate, and GS suggested that an activated intermediate was formed during the course of the reaction, despite the fact that no intermediates could be isolated [26]. Because equilibrium isotope exchange also failed to reveal an intermediate, Meister [32] suspected that both exchange and isolation were prevented because of tightly bound substrate complexes on the enzyme, ascribing an overall reversibility to the reaction mechanism. Nevertheless, a concerted mechanism was hypothesized because the products ADP and P_i do not dissociate until ammonia binds and glutamine is released [33–35]. Later, an intermediate was shown to form even in the absence of substrate NH_4^+ using a novel, scrambling isotope method called positional isotope exchange (PIX) [28,36], where a labeled ATP β-bridged oxygen ro-

[2] Also known as 5-oxoproline or pyroglutamate [5].

→

Fig. 2. Alignment of amino acid sequences of glutamine synthetases. Active-site residues (red) are conserved, suggesting a similar catalytic mechanism among different GS species. These residues are listed in Table 2. The structures of *S. typhimurium* and *E. coli* GS are known to have a common fold and to be dodecamers. Notice that the *S. typhimurium* GS sequence is relatively close to that of TB-GS, (green and orange) suggesting that TB-GS shares the same fold and oligomerization state. In contrast, human, chicken and plant GS show numerous differences from bacterial GSs (blue versus green residues). These differences are consistent with a different oligomerization state [85]. Also, notice the absence in eukaryotes of the entire adenylylation domain, including the adenylylated residue Y397 of *S. typhimurium* and *E. coli* GS (violet).

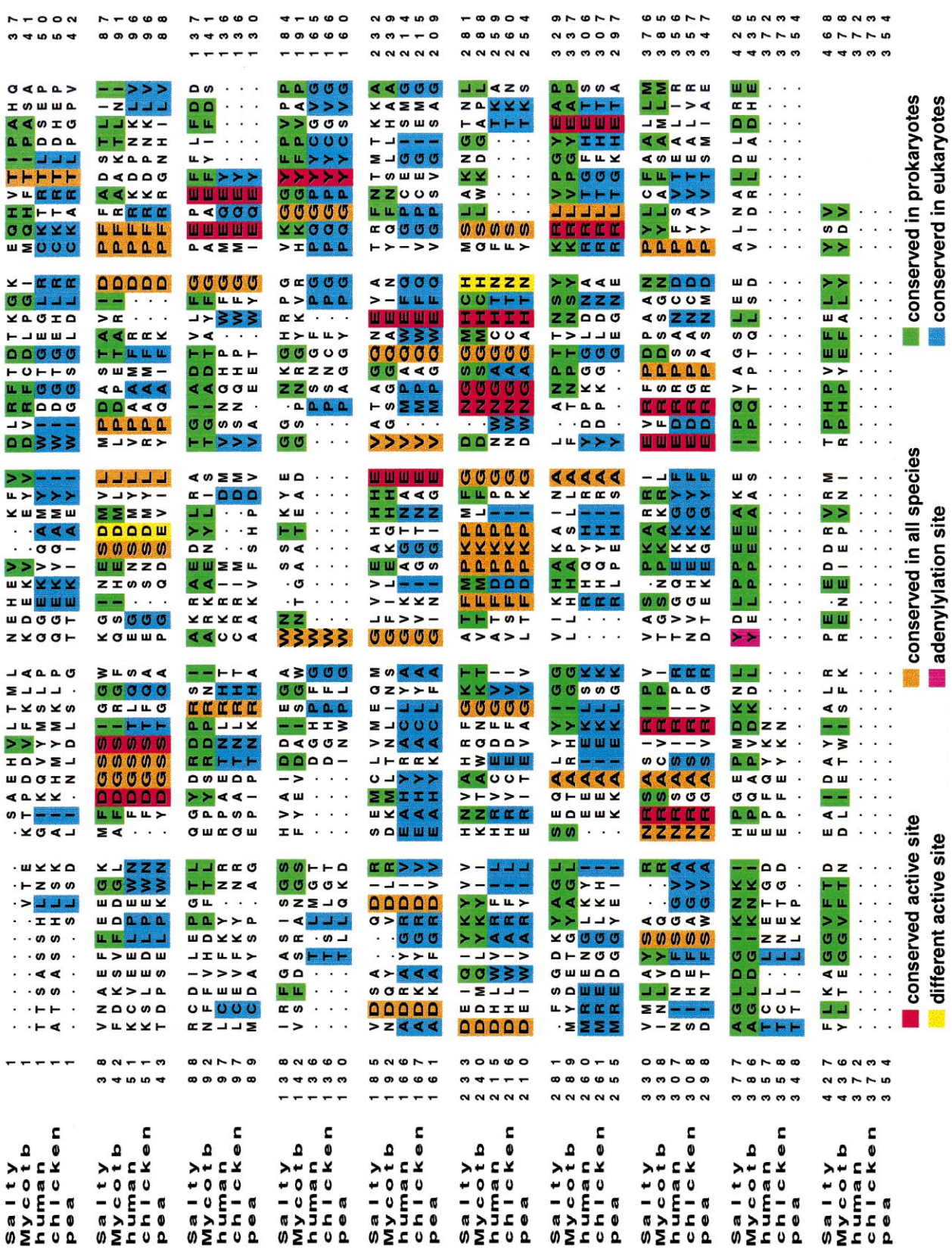
conserved active site
different active site
conserved in all species
adenylylation site
conserved in prokaryotes
conserverd in eukaryotes

tates to non-bridged oxygen positions upon phosphoryl exchanges on the enzyme.

3.1.2. L-Methionine-(S)-sulfoximine ~P inhibition

Intermediate structures in the biosynthetic reaction have been inferred and modeled from the binding of methionine sulfoximine (MetSox) [37]. MetSox competes for binding with glutamate in the active site [31,38,39]. In the presence of ATP, MetSox is phosphorylated by GS resulting in an essentially irreversible, non-covalent inhibition of the enzyme [38], apparently adopting a conformation that resembles the tetrahedral adduct at the transition state in glutamine biosynthesis [40–42]. The *S*-isomer of the MetSox sulfonimide group is the more inhibitory one [43]. The nitrogen (Nε) of the sulfonimide group receives the terminal phosphate of ATP. In an early analysis by Gass et al. [40], the methyl of the sulfonimide group was thought to occupy the ammonia binding site. This computer-assisted model suggested that this methyl group acts as an analog for substrate ammonia in the adduct, implying that ammonia is the true substrate in Reaction 1 instead of an ammonium ion. With the precise location of the attack site now known to be a negatively charged binding pocket with protein ligands placed tetrahedrally [44], an ammonium ion is now believed to be the substrate.

Other changes accompany the inhibition of GS by MetSox. The formation of the inactivation complex strengthens subunit–subunit interactions [45,46] and changes tryptophan fluorescence [47]. The inactivation of GS by MetSox is time-dependent [48–50], in that semi-log plots of activity over time (in minutes) are curved, exhibiting exponential, rather than a linear decay. Inactivation can be reversed by a variety

Table 1
Binding constants of substrates to glutamine synthetase

Substrate	K_m (mM)	Assay[a]	Species	Adenylylation state	Reference
ATP	0.58	Transfer	*S. typhimurium*	$n=0$	[57]
	0.4	forward	*E. coli*	$n=0$	[58]
	0.15	forward	*E. coli*	$n=2$	[111]
	0.68	forward	*E. coli*	Mixed	[112]
	0.13	forward	*E. coli*	$n=1.7$ or 3.3	[29]
	0.657	forward	*E. coli*	$n=12$	[111]
	1.8	other	human	n/a	[113]
	0.6	forward	plant	n/a	[114]
Glutamate	1.1	transfer	*S. typhimurium*	$n=0$	[8]
	3.3	forward	*E. coli*	$n=2$	[111]
	0.77[b]	forward	*E. coli*	$n=1.1$ or 1.8 or 8	[115]
	3.1[c]	forward	*E. coli*	$n=1.1$ or 1.8 or 8	[115]
	2.4	forward	*E. coli*	Mixed	[112]
	5.5	forward	*E. coli*	$n=0$	[58]
	6.6	forward	*E. coli*	$n=12$	[111]
	3.0	other	human	n/a	[113]
	8.2	forward	plant	n/a	[114]
Ammonium	0.1	forward	*E. coli*	$n=0$	[58]
	1.8	forward	*E. coli*	Mixed	[112]
	0.06[d]	forward	*E. coli*	$n=1.7$ or 3.3	[29]
	0.6[e]	forward	*E. coli*	$n=1.7$ or 3.3	[29]
	0.16	other	human	n/a	[113]

[a]The forward assays were typically performed at pH 7–7.5, 25°C, and contained magnesium.
[b]Measured at glutamate concentrations ranging from 0.5 to 1.2 mM.
[c]Measured at glutamate concentrations ranging from 1.2 to 2.0 mM.
[d]Measured at ammonium ion concentrations ranging from 0.25 to 1.0 mM.
[e]Measured at ammonium ion concentrations ranging from 2.0 to 10.0 mM.

of non-denaturing conditions, such as lowering the pH to 3.5–4.6 in 1 M KCl which protonates carboxylate groups, or brief heating which causes structural perturbations [45].

3.1.3. Negative feedback inhibition

The kinetic studies by Woolfolk and Stadtman [51] showed that the biosynthetic reaction catalyzed by *E. coli* GS is inhibited by nine end products of glutamine metabolism: serine, alanine, glycine, AMP, CTP, tryptophan, histidine, carbamoyl phosphate, and glucosamine-6-phosphate. Each inhibitor was found to decrease GS activity partially such that the residual activity in the presence of several inhibitors equaled the product of the individual residual activities. This was interpreted as the result of each inhibitor acting at a different site on the enzyme, distinct from the catalytic sites. Acting together the feedback-products were found almost to abolish activity. This pattern was termed 'cumulative feedback inhibition'. This conclusion was supported by double-reciprocal plots which typically demonstrated non-competitive modes of inhibition for each of the feedback products with respect to the normal substrates, but were in some cases biphasic. In retrospect, the biphasic nature of these plots may perhaps be attributed to mixed adenylylation states of GS, a phenomenon discovered later [22], or to homotropic cooperativity [9,52].

Prior to structural studies on GS, the number and nature of regulatory sites were uncertain. Separate allosteric sites for the negative feedback inhibitors were supported by methods which include fast reaction kinetics [53], equilibrium binding [54], and calorimetry [55]. However, separate sites were not supported by NMR data which suggested that the feedback inhibitors alanine, tryptophan, histidine, and glycine bound to the glutamate substrate site, at least for low- to unadenylylated GS [56]. In short, direct structural information was needed to aid in the interpretation of many solution studies of bacterial GS.

Crystal structures of GS in complex with alanine, serine, and glycine revealed that these inhibitors bind to the glutamate substrate site [8,57]. Similarly, GDP, ADP and AMP bind to the ATP site, thereby suggesting a simpler mechanism for feedback control than that of cumulative inhibition from separate sites. Liaw et al. [8] supported these conclusions by finding linear double-reciprocal kinetic plots for the inhibitors in the transferase assay using fully unadenylylated GS. However, unlike the kinetic plots from the transferase reaction, the biosynthetic reaction demonstrated more complicated behavior, still showing biphasic patterns in double-reciprocal plots. Cooperative binding effects [42,50] may be responsible for these biphasic patterns and may account for the variation of K_m values shown in Table 1 [29]. Also, consistent with the theme of cooperativity is the 2.5 Å resolution structure of GS complexed with ATP: this shows ATP has a preference for binding in an active site if the adjacent active site on the other hexameric ring has ATP bound [9,52]. This is not surprising given the extensive contacts between top and bottom layers of subunits, although the structural basis of the cooperativity is not yet known. Thus heterotropic feedback regulation of GS activity seems to be by competitive inhibition, but there is also homotropic regulation among active sites.

3.2. Transferase reaction and other arsenolysis reactions of glutamine

Another reaction commonly used as an assay of GS activity is the transferase reaction. This is a variation of the reverse of Reaction 1, in which hydroxylamine and glutamine in the presence of nucleotide, arsenate or phosphate, and metal ions yield γ-glutamylhydroxamate and free ammonia. Either ADP or ATP can support the reaction. The mechanism is thought to proceed similarly to the biosynthetic reaction in that an unstable intermediate is formed. In this case, the intermediate is γ-glutamyl arsenate. Arsenate is believed to bind at the phosphate site [29] and we speculate that the arsenate oxygen attacks glutamine. Hydroxylamine then binds at the ammonium site and attacks the intermediate thereby displacing ammonia and yielding γ-glutamylhydroxamate [31].

Other reactions catalyzed by GS are also believed to involve an intermediate. For example, hydrolysis of glutamine to glutamate and ammonia also occurs in the presence of arsenate. In the same way in which hydroxylamine attacks the intermediate and replaces arsenate in the transferase reaction, deprotonation of

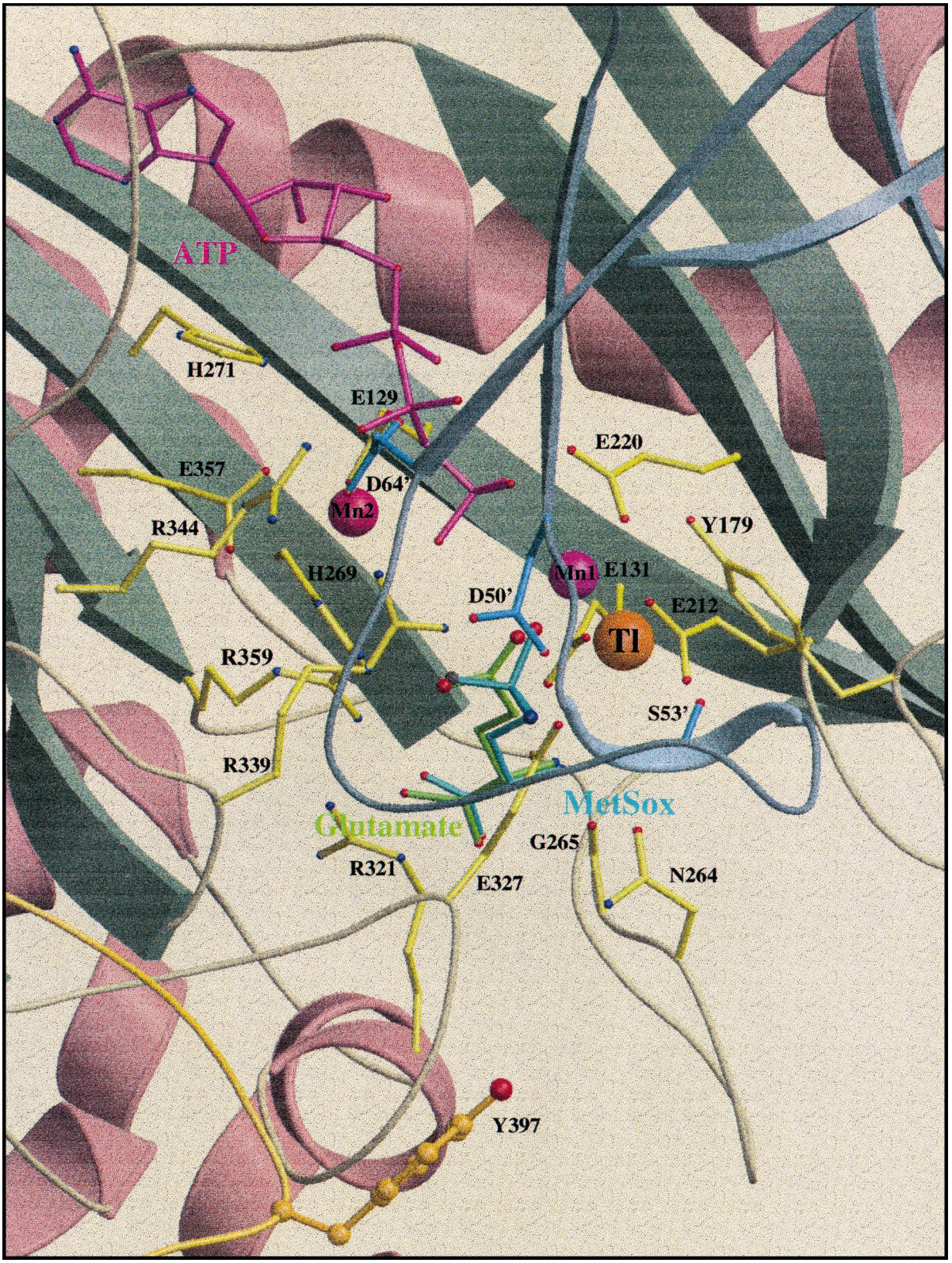
ATP
H271
E129
E357
D64'
Mn2
R344
H269
E220
Y179
Mn1
E131
D50'
E212
Tl
R359
S53'
R339
MetSox
Glutamate
G265
R321
E327
N264
Y397

a water molecule may lead a hydroxyl ion to replace arsenate in the intermediate resulting in glutamate. In summary, the ammonium ion in the biosynthetic reaction, hydroxylamine in the transferase reaction, and water in the glutamine hydrolysis reaction presumably all bind at the same (ammonium ion) site. As in the biosynthetic reaction, none of these three molecules may bind until nucleotide has bound and the corresponding intermediate is formed [31]. The cooperative effect of binding is the subject of the following section.

4. Structure–function relationships

4.1. Side-chain movements of key active site residues

Local conformational changes and side-chain movements in active site residues have been described for GS crystals soaked in solutions with ligand [8,11,31,57]. These residues are absolutely conserved among GS in both lower and higher organisms (Fig. 2) and appear to play key roles in the mechanism of the biosynthetic reaction. Table 2 lists all the active site residues, including their suggested roles in the reaction mechanism. The following describes the most prominent structural changes and their effectors.

4.1.1. Effects on the Glu-327 flap by MetSox binding

Glu-327 is part of a loop, termed 'the Glu-327 flap' consisting of residues 323–330, that guards the glutamate entrance to the active site. The Glu-327 flap closes the active site, shielding the γ-glutamyl phosphate intermediate from aberrant hydrolysis. When the flap is closed, the Glu-327 carboxylate forms part of the ammonium site [11,31]. Asp-50′[3] deprotonates the ammonium ion, forming ammonia. Ammonia attacks the γ-glutamyl phosphate intermediate thereby forming a tetrahedral intermediate at the transition state. The Glu-327 flap accepts a proton from the δ-amino group of the tetrahedral intermediate, yielding glutamine [31,58]. The Glu-327 flap is not normally seen in the native-GS electron density maps nor in the difference maps of glutamate–, alanine– or glycine–GS complexes. The function of Glu-327 has mainly been inferred from difference maps of MetSox–GS and PPT–GS complexes [11,31].

The Glu-327 flap also explains the extremely tight binding of the MetSox∼P[ADP] complex to GS because the Glu-327 flap is positioned by MetSox to block the entrance to the glutamate binding site [11,31]. In this closed position, the flap may interact with Ser-52′ or Ser-53′ of the adjacent subunit, thereby providing the increase of inter-subunit stabilization which has been noted during MetSox binding [45,46].

4.1.2. Effects on the Asp-50′ loop by nucleotide binding

Asp-50′ is part of a loop located on the N-terminal domain (residues 1–100). Each active site is formed at the interface between the C-terminal domain (residues 101–468, see Fig. 1) of one subunit and the N-terminal domain of an adjacent subunit within a dodecameric ring. Most of the active site is formed by residues of the C-terminal domain. Asp-50′ is in the N-terminal portion of the active site. Asp-50′ is believed to bind the ammonium substrate and then to accept a proton from ammonium, resulting in the formation of ammonia which is now poised to attack the phosphorylated-glutamyl intermediate [31].

The position of Asp-50′ is controlled by nucleotide binding. Both ADP and ATP enter the active site from the top of the bifunnel, with the phosphate chain pointing into the bifunnel. The presence of ADP induces Arg-339 interaction with Asp-50′ and

←
Fig. 3. Residues in the active site of GS. Superimposed in the figure are models of the substrates ATP (violet), glutamate (light green), MetSox (aqua), and the Tl^+ ion (orange) occupying the NH_4^+ substrate site in the active site. The green β-sheets, the pink helices and the yellow side-chain loops represent the C-terminal domain of one subunit, and the blue secondary structures represent the N-terminal domain of the adjacent subunit. The residues described in Table 2 are shown here. Several of the key residues (Glu-327, Asn-264, Asp-50′) lie in loops which comprise the active site. The adenylylation loop is shown in orange (at lower left).

[3] The symbol ′ indicates that the residue belongs to the adjacent subunit.

Table 2
Active site/catalytic residues

Residue	Role in enzymatic mechanism	Effector	Reference
Asp-50	Depronates the ammonium substrate ion. Increases the affinity for ammonium binding	ADP	[31,44,58]
Ser-53	Increases intersubunit stability by interacting with Glu-327	ADP	[31]
Asp-64[a]	Increases intersubunit stability by interacting with Arg-344	ADP	[57]
Glu-129	Coordinates the n2 ion and hydrogen bonds with His-271		[31]
Glu-131	Coordinates the amino group of glutamate and the n1 ion		[31]
Tyr-179	Coordinates the ammonium binding pocket		[31,44]
Glu-212	Coordinates the ammonium binding pocket and the n1 ion		[31]
Glu-220	Coordinates the n1 ion		[31]
Asn-264	Coordinates the amino group of glutamate. Stabilizes the Glu-327 flap upon MetSox or PPT binding	Glu, Gln, Ser, Gly, Ala, Tl^+, PPT, MetSox	[11,31]
Gly-265	Coordinates the amino group of glutamate		[31]
His-269	Coordinates the n2 ion		[24,117]
His-271[b]	Coordinates the α-phosphate group of ADP/AMPPMP and Glu-129		[57]
Arg-321	Coordinates the carboxylate of glutamate		[31]
Glu-327	Stabilizes the tetrahedral adduct at the transition state. Accepts a proton from the adduct to form glutamine. Closes active site and shields intermediate from hydrolysis	Ser, Tl^+, PPT, MetSox	[8,11,31,44,58]
Arg-339	Induces intersubunit stability by interacting with Asp-50	ADP	[31]
Arg-344	Coordinates the β-phosphate group of ADP/AMPPMP	ADP	[31]
Glu-357	Coordinates the n2 ion and Arg-344	ADP, AMPPMP	[31]
Arg-359	Coordinates the γ-carboxylate group of glutamate		[31]
Tyr-397	Site of adenylylation (seen in bacterial GS only)		[6]

The residues listed here are strictly conserved among prokaryotic and eukaryotic GS, as shown in Fig. 2. All of these residues line the active site cavity except for adenylylation residue Tyr-397 which sits on a loop outside and below the bifunnel. Based on X-ray crystallographic studies [6,11,31,44] and much earlier biochemical work in the literature, including the kinetic studies of Colanduoni et al. [116], all residues listed here are believed to play key roles in catalysis or binding of substrates and other ligands. Fig. 3 illustrates the relative positions of these residues in the active site and Fig. 4 demonstrates how key active site residues function to synthesize glutamine.

[a]Change to glutamate in pea GS.

[b]Change to asparagine in eukaryotic GS.

induces Arg-344 interaction with Asp-64′ [57], providing additional contacts for inter-subunit stabilization within a ring. The movement of Asp-50′ aids in the formation of the ammonium binding site, and the movement of Arg-339 may assist phosphoryl transfer and P_i binding. ADP binding also increases the affinity for substrate glutamate by inducing Arg-359 movement toward one of the γ-carboxylate oxygens of substrate glutamate. The movement is manifested in the enhancement of dissociation constants [31,59]. Finally, the β-phosphate of ADP shifts Glu-129 toward the n2 ion, His-269, and His-271 [57]. Collectively, these movements illustrate how nucleotide binding increases the affinity for the subsequent binding of substrates and are consistent with an ordered, sequential mechanism of glutamine synthesis.

4.1.3. Effects on the Asn-264 loop by glutamate analogs

Asn-264 resides on a flexible loop (residues 255–266) near the glutamate entrance at the lower end of the bifunnel and is adjacent to the Glu-327 flap [11]. In the native structure, Asn-264 occupies the site to which the amino group of the substrate glutamate will bind [31]. Upon glutamate binding, the side chain swings away toward the ε-amino group of Lys-176 [8]. This is also true in the alanine, glycine, and glutamine complexes with GS [8]. In thallium–GS complexes [11,44], Asn-264 is one of the coordinating ligands for a second negatively charged pocket which binds a Tl^+ ion. This polar pocket may be a second ammonium site. In the biosynthetic reaction, this second site serves to position the amino group of

substrate glutamate in the active site and provide for its stabilization. In MetSox–GS complexes, Asn-264 moves away from this site to help MetSox stabilize the Glu-327 flap [11,31]. This is also true in serine–GS complexes, where Asn-264 stabilizes the Glu-327 flap with the aid of the hydroxyl group of serine [8]. The function of the Asn-264 residue in the biosynthetic reaction may therefore be to close the flap [11]. It is likely that Asn-264 is triggered by the amino group of glutamate to aid Ser-53′ in flap closure, allowing both Asn-264 and Ser-53′ to interact with the side chain of Glu-327.

4.2. Enzymatic mechanism of bacterial GS

The reaction mechanism can be described as a series of loop and side-chain movements, based on crystal structures of enzyme–ligand complexes from Liaw and Eisenberg [31] and Gill et al. [11], reflecting intermediate states. The mechanism can be followed in Fig. 4: (a) ATP binds within the top of the bifunnel, its terminal phosphate group binding adjacent to the n2 ion. The binding of ATP results in the movement of the Asp-50′ loop, which is represented by the motion of the Asp-50′ side chain toward the site to which an ammonium ion will subsequently bind. Arg-359 (not shown) also moves toward the site to which the γ-carboxylate group of glutamate will subsequently bind. Both these movements increase the affinity for glutamate and ammonium binding; (b) glutamate enters the cavity from the bottom-side of the bifunnel and binds above the Glu-327 flap, its

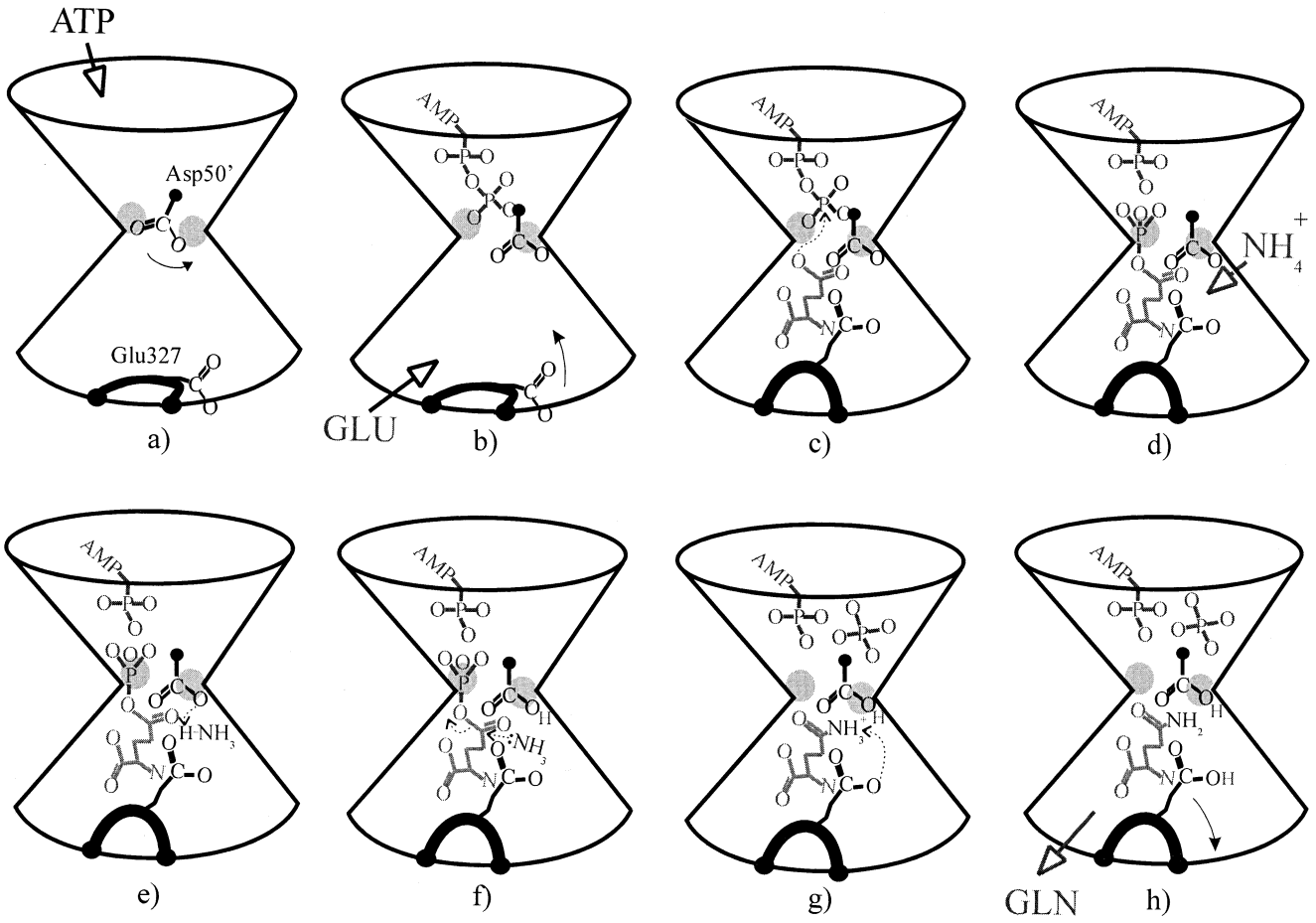

Fig. 4. Illustration of glutamine biosynthesis by GS. A cartoon of one active site of GS suggests the mechanism of glutamine synthesis. At the neck of the bifunnel sit the n1 and n2 metal ions shown as gray balls. Catalytic residues, including Asp-50′ which rotates and Glu-327 on the loop called the Glu-327 flap, are shown in black. Substrates (dark gray) enter from the top (ATP) and bottom (glutamate). The binding of substrates, motion of loops, and catalysis are illustrated in the consecutive images. The mechanism is described in the text.

γ-carboxylate group binding adjacent to the n1 ion. The amino group of glutamate shifts the Asn-264 loop (not shown), aiding Ser-53′ (not shown) on the Asp-50′ loop, to stabilize the flap. The active site is now closed and is shielded from water, and the ammonium binding site is complete; (c) the γ-phosphate of ATP is transferred to the γ-carboxylate of glutamate, thereby forming the intermediate. The two positively charged metal ions and Arg-339 participate in phosphoryl transfer by polarizing the γ-phosphate group of ATP making the γ-phosphorus more positive; (d) an ammonium ion enters the bifunnel and binds at the negatively charged pocket created by Glu-327, Asp-50′, Tyr-179, Glu-212, and Ser-53′ (the last of these residues not shown); (e) the side chain of Asp-50′ deprotonates the ammonium ion, forming ammonia; (f) ammonia attacks the δ-carbon of the γ-glutamyl phosphate intermediate, thereby releasing the phosphate group. A salt-bridge is now formed between the tetrahedral adduct and Glu-327; (g) Glu-327 accepts a proton from the adduct, thereby neutralizing the salt-bridge and forming glutamine; and (h) the Glu-327 flap opens and glutamine is released.

5. Eukaryotic glutamine synthetase

Prokaryotes and eukaryotes were once thought to express different forms of glutamine synthetase: Prokaryotes expressed GS I, while eukaryotes expressed GS II. More recently, it has been reported that GS II is also present in some bacteria, although, GS I has not been found in any eukaryote [60]. Bacterial type I GS is a 12-subunit complex whose three-dimensional structure is known ([6] and Section 2 of this review). The three-dimensional structure of type II GS is not yet known. GS IIs have a polypeptide chain of ∼372 residues, which is distantly related to GS I (Fig. 2). Unlike the dodecameric GS I, GS II has been reported to exist as an eight-subunit oligomer [61]. Type I and type II forms of GSs have some, but not all, of their effectors in common. All identified active site residues of GS from the type I structure are invariant among all species (Table 2) (see also [60]), therefore the mechanism of action must be similar [62].

There is a wealth of literature about GS I, but few publications about GS II. The main focus of research on GS II for the last 40 years has been on GS from brain of various animals. The interest in human brain GS stems from in illnesses such as Schizophrenia, Parkinson's disease [63], Huntington's chorea [64], Alzheimer's disease [65] and the fact that it is overexpressed following brain injury [66]. Most of the biochemical properties have been established using enzyme derived from sheep brain [67]. Forty years of studies of the enzymology of eukaryotic GS have included work on the following tissues: rat liver [68–70], rabbit and rat skeletal muscle [71], pig brain [72,73], bovine brain [74–76] and human brain [77–79], as well as many studies on sheep brain [61,67,75,80–87].

For reviews on eukaryotic GS see Meister [71], Wedler and Denman [88], Wedler and Toms [4] and Purich [5].

5.1. Regulation of eukaryotic GS

5.1.1. Regulation by expression

The expression of the glutamine synthetase gene in *E. coli* is highly regulated by nitrogen starvation. Full expression requires growth in a nitrogen limited environment [3]. Although this is not observed for GS II, it has been reported that hormones, such as insulin and hydrocortisone, can induce changes in the rate of GS II biosynthesis [71,89,90]. The multiple GS II genes of higher plants are differentially expressed in vivo, and each encodes a distinct GS polypeptide which is targeted to subcellular compartments (chloroplast or cytosol) [91].

5.1.2. Regulation by metal ions

Like the bacterial GS I, the eukaryotic GS II requires two divalent metal ions per subunit for activity [74]. The higher affinity site n1, binds manganese Mn(II) or magnesium Mg(II). These ions have a structural as well as a catalytic role. The lower affinity site n2, is occupied by a metal bound nucleotide, essential for activity [76]. Type II GS exhibits regulatory effects and the enzyme is active in vitro with a number of divalent metal ions, although the specific activity and the pH optimum varies considerably depending on the metal ion present [82]. Human and sheep GS from brain are 10 times more active with Mg(II) bound than with Mn(II) [77,80], even though

the enzyme has 300–1000 times higher affinity for Mn(II) than for Mg(II) [92]. The eukaryotic enzyme is most active in mM concentrations of Mg(II), but μM concentrations of Mn(II) will decrease the activity even in the presence of mM Mg(II).

There has been much discussion of the metals found in GS II. Wedler and coworkers proposed that GS II is a Mn(II) containing enzyme [85], whereas Ginsburg and coworkers found that GS binds Mg(II) instead [74,76]. Wedler and Ley reported later [93], that the concentration of free cytoplasmic Mn(II) in chicken brain cells is near the K_d for the GS–Mn(II) complex [87,93]. In the presence of mM Mg(II) and μM Mn(II), 20–30% of GS subunits were trapped with bound Mn(II) [93]. This suggested that Mn(II) is indeed physiologically important in the regulation of GS. Kinetic studies further indicated that Mg(II) ions enhance the affinity of GS for Mn(II) ions [93], raising the possibility of synergistic interaction between the metal ion sites of GS.

5.1.3. Regulation by association–dissociation

The type II GS has been reported to be regulated in vitro by association and dissociation of subunits [86]. Mn(II) or Mg(II) concentrations, presence of substrates and enzyme concentration of sheep brain GS can change the oligomeric state in vitro from inactive monomer to tetramers (estimated specific activity of 172 U/mg), to octamers (200 U/mg, $K_d = 2.5 \times 10^{-6}$ at 37°C) to a highly active octameric form (900 U/mg, Mn(II)-activated). At protein concentrations below 4 μg/ml (20 nM octamer) the oligomer dissociates into tetramers and then into inactive monomers [86]. Lanthanide ions in high concentrations can force a single GS octamer to associate further to an oligomeric species of more than five octamers. Mg(II), however, affects only the tetramer–octamer transition even at high concentrations [86]. At the concentrations of sheep brain GS at which tetramer predominates, addition of substrates alone or in pairs causes partial reassociation to octamers, the most effective being ATP and glutamate, ADP and L-glutamine, or ATP and MetSox [86]. It is still not clear whether Mn(II)-dependent oligomerization of GS octamers into higher oligomers is physiologically important, because of the relative high concentrations of Mn(II) required.

5.1.4. Regulation by effectors

Type II GS acts on both L- and D-glutamate and certain glutamate analogs (e.g. β-glutamate, *cis*-cycloglutamate, and α-methyl-L-glutamate), is essentially irreversibly inhibited by MetSox, and is inhibited by carbamoyl phosphate in the presence of Mn(II), but not Mg(II) [70].

There are tissue-specific differences in the regulatory properties of mammalian GS: GS from liver is regulated by various pathway metabolites [68–70]. The liver enzyme responds very differently than brain GS to feedback inhibition by metabolites derived from L-glutamine. The liver enzyme is inhibited by glycine, L-alanine, L-serine, L-glutamine, L-histidine, and carbamoyl phosphate in the presence of Mn(II), but not Mg(II), and is activated by α-ketoglutarate and citrate [62,71]. In contrast, brain GS is inhibited by carbamoyl phosphate in the presence of Mn(II), but does not respond to physiological levels of other feedback modifiers or end-product metabolites derived from L-glutamine. In vitro studies with sheep brain GS showed that activation or inhibition (e.g. by α-ketoglutarate or by glycine, respectively) is relatively slight and requires high concentrations (100 mM) of the effectors [69]. Brain GS from all species investigated shows a similar inhibition profile. The difference in response to effectors of GS in various tissues must reflect their functional roles in these tissues.

In the brain, GS is an enzyme of primary neurochemical importance, since it converts neurotoxic ammonia and the neurotransmitter L-glutamate into L-glutamine. The neurotransmitter L-glutamate is incorporated into vesicles at the neuronal synaptic junction and is released upon stimulation. It is then converted into L-glutamine and recycled into the neuron vesicles. No net glutamate is actually consumed, just recycled.

In other tissues GS II is important for biosynthesis or nitrogen metabolism. Both glutamate and glutamine are used for protein synthesis, but glutamine is also an ammonia donor for various biochemical pathways. Therefore, low concentrations of glutamine-dependent metabolites should stimulate GS activity and high concentrations of these end products should inhibit it. This is what is observed: non-brain GS responds to end-product feedback inhibition, whereas brain GS does not [69].

There are contradictory reports regarding GS II inhibition with ADP. Rat skeletal muscle GS has been reported to be markedly inhibited by ADP unlike the brain and liver enzymes [71], although suppression of activity by ADP has been reported for the human [77] and sheep brain [80] enzyme: at a 1:1 ratio of ADP/ATP, the inhibition is less prominent for the human enzyme (50%) than for the sheep enzyme (80%) [77].

Allosteric sites on GS II have been proposed for arsenate and L-glutamate [76] and for two more Mn(II) ions per subunit [86]. Another ion which affects the activity of GS is the chloride anion (Cl^-). In enzyme assays, this anion behaves as if it has a tight binding site on each subunit of GS and induces considerable structural perturbations upon binding [76]. In the presence of Cl^-, the affinity of the enzyme for Mn(II) or Mg(II) increases 2–4-fold. GS II is also likely to be in a Cl^--rich environment at all times, which would affect the in vivo enzymatic properties of GS II.

5.1.5. Regulation by modification

While there are many indications that the catalytic mechanisms of eukaryotic and bacterial GS are fundamentally similar, their regulation is different. Bacterial GS I is regulated by feedback inhibition and covalent modification (see Sections 2 and 3) when the bacterial cell enjoys an excess of the nitrogen containing end products of glutamine metabolism [1]. The shorter sequence of GS II lacks the adenylylation loop (Fig. 2). No significant enzyme-level regulatory mechanism for eukaryotic GS II has been reported to date. Inactivation of sheep brain GS by ADP-ribosylation of an active site arginine residue by NAD:arginine ADP-ribosyltransferse from turkey erythrocytes has been reported [94]. However, whether this reaction is of physiological significance and whether this or a similar enzyme is found in the brain is yet unclear [92].

In summary, there seem to be two classes of eukaryotic GS, the enzyme isolated from brain and enzyme isolated from other tissues, because of the different behavior regarding feedback regulation [69]. Because the GS molecules isolated from different tissues of the same species are identical in sequence yet different in biochemical properties, there must be some post-translational modification. Further studies are necessary to shed light on the different ways these enzymes are regulated and modified.

5.2. Half-site reactivity

Sheep brain GS has been reported to have four tightly bound Mn(II) per octamer [85]. In contrast, bovine brain GS has been reported in vivo to contain 16 bound Mg(II) per octamer, but no tightly bound Mn(II) [76]. Mn(II) appears to bind in a competitive manner versus Mg(II) in vitro [92]. Different researchers working on type II GS have proposed a model in which the eight subunits of GS exhibit a strong negatively cooperative interaction or half-site reactivity [73,86], induced by Mn(II) binding and inactivation by MetSox [88]. While some groups have reported four to six ligands per octamer in MetSox-inactivated sheep brain or rat liver enzyme [69,92], Ginsburg's group has found that in agreement with early papers on sheep GS [38,48,95], the bovine brain enzyme could bind up to eight equivalents each of ADP and MetSox$\sim$P and 16 divalent cations per octamer [76]. This finding contradicts the proposed half-site reactivity model.

5.3. Biophysical and biochemical properties

5.3.1. Specific activity

Specific activities reported for the eukaryotic enzyme range from 10 U/mg for pig brain [73], 134 U/mg for rat liver [70], 179 U/mg for human brain GS [77], 200 U/mg for sheep brain GS [92] to 400 U/mg for bovine brain GS [75]. An activated form of sheep GS was reported to have a specific activity of $\sim$900 U/mg [86]. Although this wide range of specific activities could be due to species or organ differences, they instead were mostly found to be due to differences in protocols for purification and determination of protein concentration. With different estimated protein concentrations, the turnover rate, as well as the stoichiometry of effector binding and negative cooperativity appear different [92]. Wedler proposed that the use of EDTA in the purification is responsible for the range in specific activities of earlier reports. In addition, the protein concentration is not easy to determine accurately, as discussed in the next section. Type II GS purified by Maurizi et al. [75] showed a specific activity of 400 U/mg for the bovine

Table 3
Synthetic inhibitors of glutamine synthetase

Structure	Commments
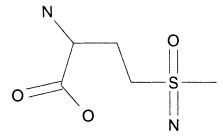 methionine sulfoximine (MetSox)	Very potent ATP-dependent inactivator of GS from most species. First discovered in nitrogen chloride treated zein [106]. Ki = 105μM (sheep brain) [118], 1μM (*E.coli*) [119], 161μM (pea leaf) [120], 100μM (spinach) [107]
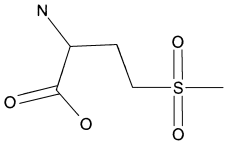 methionine sulfone	Synthetic inhibitor related to MetSox [48]
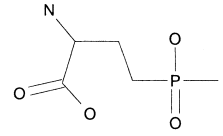 phosphinothricin (PPT)	Very potent ATP-dependent inactivator of GS from most sources. Produced as part of a tripeptide antibiotic by *Streptomyces viridochromogenes* [121]. Ki = 25.2μM (sheep brain) [122], 1.6μM (*E.coli*) [123], 8μM (sorghum seed), 0.22μM[1] (mung bean) [124], 1.5μM (spinach leaf) [125], 320μM (rat liver) [108], 73μM (pea leaf) [120]
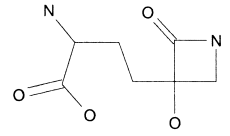 tabtoxinine-β-lactam	Very potent GS inactivator produced by *Pseudomonas* pv. *tabaci* [109]
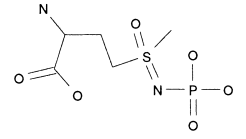 methionine sulfoximine phosphate	Potent synthetic transition-state mimic derived from MetSox [95].
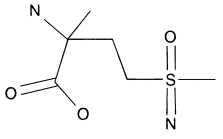 alpha-methyl methionine sulfoximine	Slightly less inhibitory synthetic MetSox derivative [126]. This and the five α- and γ-substituted MetSox derivatives that follow are ordered by decreasing potency.

Table 3 (*continued*)

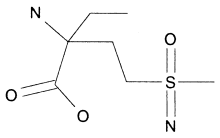 alpha-ethyl methionine sulfoximine	[126]
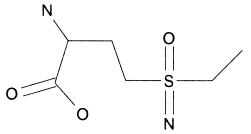 ethionine sulfoximine	[127]
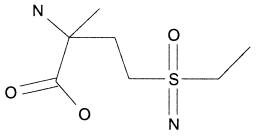 alpha-methyl ethionine sulfoximine	[127]
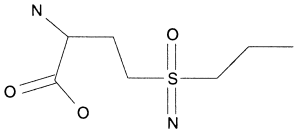 prothionine sulfoximine	[127]
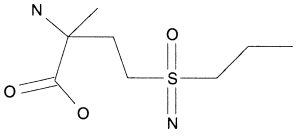 alpha-methyl prothionine sulfoximine	[127]
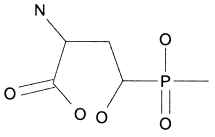 gamma-hydroxy phosphinothricin	Synthetic inhibitor with Ki = 47μM (sheep brain) [118], 1.6μM (*E.coli*) [123], 14μM (sorghum seed) [128], 0.22μM[1] (mung bean) [124], 6μM (spinach leaf) [125]
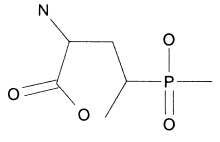 gamma-methyl phosphinothricin	Synthetic inhibitor with Ki = 407μM (sheep brain) [118], 25μM (*E.coli*) [123], 67μM (sorghum seed) [128], 140μM[1] (mung bean) [124], 123μM (spinach leaf) [125].

Table 3 (*continued*)

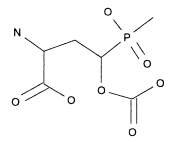 gamma-acetoxy phosphinothricin	Synthetic inhibitor with Ki = 33μM (*E.coli*) [123], 178μM (sorghum seed) [128].
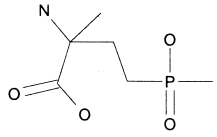 alpha-methyl phosphinothricin	Synthetic PPT derivative. Ki = 125μM (sheep brain) [122], 5.7μM (*E.coli*) [119], 12μM (sorghum seed) [125], 8μM (spinach leaf) [125], 56μM (rat liver) [108]
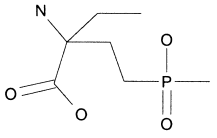 alpha-ethyl phosphinothricin	Synthetic inhibitor with Ki = 111μM (sheep brain) [122], 11.2μM (sorghum seed), 16μM (spinach leaf) [125].
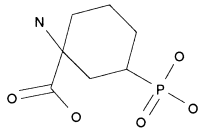 cyclohexane phosphinothricin	Synthetic inhibitor with Ki = 125μM (sheep brain) [122], 24μM (*E.coli*) [119], 10μM (sorghum seed) [125], 310μM[1] (mung bean) [124], 36μM (spinach leaf) [125].
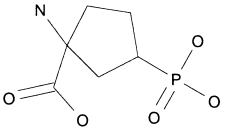 cyclopentane phosphinothricin	Synthetic inhibitor with Ki = 0.47μM[1] (mung bean) [124].
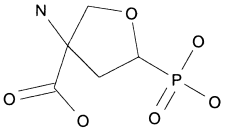 tetrahydrofuran phosphinothricin	Ki = 5μM[1] (mung bean) [124]
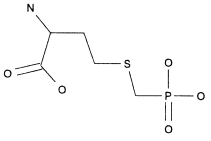 s-phosphonomethyl homocysteine	Synthetic compound with "measurable inhibition of sheep brain GS" [129].

Table 3 (*continued*)

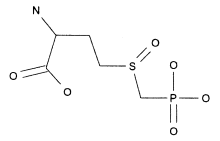 s-phosphonomethyl homocysteine sulfoxide	Synthetic compound with "measurable inhibition of sheep brain GS" [129].
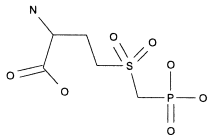 s-phosphonomethyl homocysteine sulfone	Synthetic inhibitor with Ki = 1.4mM (sheep brain) [129].
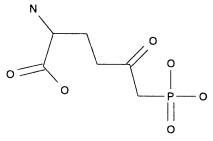 4-(phosphonoacetyl)-L-alpha-aminobutyrate	Synthetic inhibitor with Ki = 660μM (sheep brain), 4.8mM (*E.coli*), 590 μM (pea seed) [130].
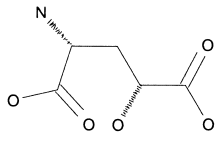 threo-4-hydroxy- D-glutamic acid	Synthetic glutamic acid derivative with Ki = 1.5mM (*Chlorella pyrenoidosa*) [131].
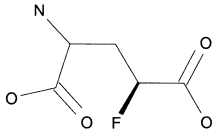 threo-4-fluoro- D,L-glutamic acid	Synthetic glutamic acid derivative with Ki = 0.8mM (*Chlorella pyrenoidosa*) [131].
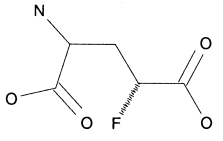 erythro-4-fluoro- D,L-glutamic acid	Synthetic glutamic acid derivative with Ki = 2mM (*Chlorella pyrenoidosa*) [131].
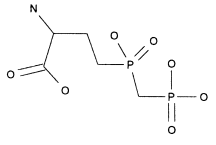 2-amino-4-[(phosphonomethyl) hydroxyphosphinyl] butanoic acid	Synthetic inhibitor with Ki = 750μM (sheep brain), 75μM (*E.coli*), 250μM (pea seed) [132].

Table 3 (*continued*)

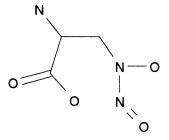 Alanosine	Antibiotic produced by *Streptomyces alanosinicus*. Ki = 1.3mM (mouse liver), 4mM (mouse brain) [133].
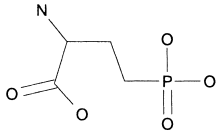 2-amino-4-phosphono butanoic acid	Synthetic inhibitor with Ki = 54μM (*E.coli*) [29], 880μM (rat liver) [108], 600μM (pea GS2) [107].
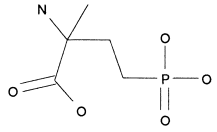 2-amino-2-methyl-4-phosphono butanoic acid	Synthetic inhibitor with Ki = 6.3mM (rat liver) [108].
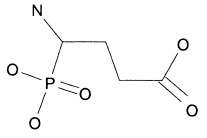 4-amino-4-phosphono butanoic acid	Synthetic inhibitor with Ki = 1.3mM (rat liver) [108].
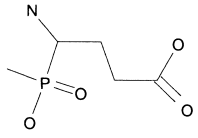 4-amino-4-(hydroxymethylphosphinyl) butanoic acid	Synthetic inhibitor with Ki = 790μM (rat liver) [108].
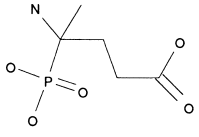 4-amino-4-methyl-4-phosphono butanoic acid	Synthetic inhibitor with Ki = 16mM (rat liver) [108].
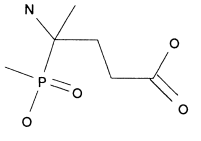 4-amino-4-(hydroxymethylphosphinyl)-4-methyl butanoic acid	Synthetic inhibitor with Ki = 9.5mM (rat liver) [108].

Table 3 (*continued*)

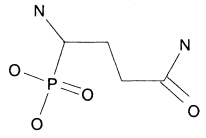 4-amino-4-phosphono butanamide	Synthetic inhibitor with Ki = 5.5mM (rat liver) [108].
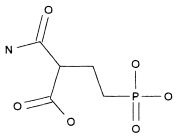 2-amido-4-phosphono butanoic acid	Synthetic inhibitor with Ki = 6.2mM (rat liver) [108].
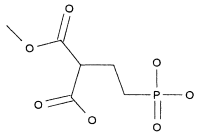 2-methoxycarbonyl-4-phosphono butanoic acid	Synthetic inhibitor with Ki = 8.7mM (rat liver) [108].
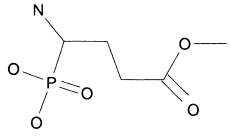 methyl 4-amino-4-phosphono butanoate	Synthetic inhibitor with Ki = 2.1mM (rat liver) [108].
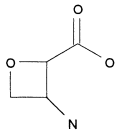 oxetin	Antibiotic produced by *Streptomyces* sp. with Ki = 1.2mM (*B.subtilis*), 3.4mM (spinach leaf) [134].
IF7 and IF17 polypeptides	Natural peptidal inhibitors of *Synechocystis* sp. GS [135]
110 kD Protein	A macromolecular inhibitor of GS found in tomato roots [136].

Table 3 (*continued*)

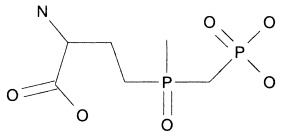 (3-amino-3-carboxypropyl)-(phosphonomethyl) phosphinic acid	Synthetic derivative of PPT with Ki = 2.2mM (pea GS2) [107].
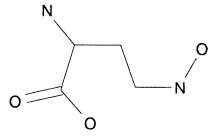 N-hydroxy-L-2,4-diaminobutyrate	Synthetic inhibitor with Ki = 7μM (sheep brain), 21μM (soybean) [137].
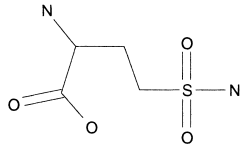 3-amino-3-carboxypropane-sulfonamide	Synthetic inhibitor with Ki = 51μM (*E.coli*) [29].
Various CBZ-, PA- and PP- amino acid derivatives	A number of carbobenzoxy (CBZ) [138], phenylacetyl (PA) and 3-phenylpropionyl (PP) [139] found to be inhibitors of sheep brain GS
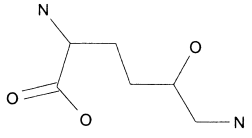 5-hydroxylysine	Amino acid found in collagen. First used as an inhibitor of glutamine and protein synthesis in carcinoma cells [140]. Ki = 490μM (maize GS1), 850μM (maize GS2) [114], 40μM (*S. typhimurium*) (Rotstein, S.H. and Eisenberg, D., unpublished data).

The following references have been cited in the table: [29, 95, 106–109, 114, 118–140].

[1]Inhibition constants for mung bean glutamine synthetase were given as Ki* = Ki *(K_{react}/K_{inact}), where K_{react} and K_{inact} are, respectively, the enzyme reactivation and inactivation rate constants [124].

brain enzyme and 300 U/mg for the sheep brain enzyme, similar to the later corrected values by Wedler [92], but different from earlier reports. Even recent studies on human brain GS report a low specific activity of about 170 U/mg [79]. This is likely due to following the original purification protocols which include EDTA [67].

5.3.2. Absorption coefficients

The measured specific activities depend on the purification method used and on the protein concentration, usually determined by calibrated protein assays or spectrophotometrically at wavelength 280 nm. The published absorption coefficients differ for each species and for each publication: Reported are values for bovine brain GS $A^{0.1\%}_{280\ nm,\ 1\ cm} = 1.5$ [75], for sheep brain GS $A^{0.1\%}_{280\ nm,\ 1\ cm} = 1.35$ [83], $A^{0.1\%}_{280\ nm,\ 1\ cm} = 1.14$ [92], and $A^{0.1\%}_{280\ nm,\ 1\ cm} = 0.61$ [85], and for pig brain GS $A^{0.1\%}_{280\ nm,\ 1\ cm} = 11.1$ [72]. These values might not be accurate, considering that binding of ATP,

Mn(II) or Mg(II) can change the absorption at 280 nm [76], and these effector concentrations may be different for each protein purification. These might also result in overestimating the protein concentration in binding studies with ATP and MetSox. Protein concentrations are usually determined by the microbiuret assay procedure of Layne [96] or the Coomassie dye method of Bradford [97], which are not very accurate and can be affected by EDTA [92]. Protein concentration has been more accurately determined by spectrophotometric absorption by the group of Ginsburg [75], using Rayleigh optics and the method of Babul and Stellwagen [98] to measure the extinction coefficient.

5.3.3. Molecular weight determination

Another discrepancy in studies of GS II is its molecular weight, which ranges in reports from 352 kDa for rat liver GS [70], 370 kDa for pig brain GS [72], 430, 497 and 525 kDa for sheep brain GS [81,83], to 520 kDa for pea leaf cytosol GS [99]. Based on electron micrographs, it has been postulated that GS II is an octamer that consists of two stacked tetramers with D4 symmetry [72]. Some of the earlier estimates for the molecular weight of GS II oligomer have come from direct measurements (gel filtration, sedimentation). Current molecular weight estimates are often calculated by multiplying the monomer molecular weight (from sequence) by the generally accepted number of subunits (eight from micrographs). Early monomer molecular weights, on the other hand, before the sequence was known, seem to be estimated by dividing the measured complex weight by eight. The monomer molecular weight determined from sequence ($M_r \sim 42$ kDa) is much smaller [91,100,101], than the values given in earlier papers [72,83,99]. Based on sedimentation experiments (velocity and equilibrium) and knowledge of the monomer molecular weight, the calculated number of subunits for the GS II complex varies from the generally agreed eight: GS II consists of 11 subunits in pea seed cytosol [99], nine subunits in pig brain [72], 10–13 subunits in sheep brain [81,83] and 11 subunits in human GS (Pfluegl, G.M.U, unpublished results). The difference in number of subunits determined by sedimentation or by electron micrographs is to date not explainable, although it has been pointed out that interpretations of analytical ultracentrifugation, gel filtration and negative staining electron microscopy studies of oligomeric protein subunit stoichiometry are often ambiguous [102].

In bacterial GS, the active site lies between two adjacent subunits in a ring of six. To preserve this fundamental feature in GS II, the halves of active sites must be adjacent to each other. Homology modeling of human glutamine synthetase indicates that a tetramer would have an open structure, with two complete active sites and two open non-functional sites per tetramer ([103] and Pfluegl et al., unpublished data), making the half-site active model more attractive than a closed form [104]. But one study by Maurizi et al. [76] showed that all active sites were active and able to bind ligands. Nevertheless, attempts to reconstitute stabilized submolecular oligomers (e.g. dimers, trimers) of the human brain GS II (as done with bacterial GS [45,105]) were unsuccessful. It is clear that the inconsistencies among various studies of the mass and subunit arrangement in GS II demand a reinvestigation of the structure, using current biophysical tools.

6. Synthetic inhibitors of glutamine synthetase

The inhibition of glutamine synthetase has been studied extensively. Inhibitors of GS have been used to establish the kinetic mechanism of the enzyme, to characterize the regulation of GS in vivo and to assess the systemic effect that inhibition of glutamine production has on different organisms. In this section, we focus on compounds, either natural or synthetic, designed primarily for the inhibition GS. Regulatory inhibitors (covalent and feedback) are discussed in Sections 3 and 5.

GS has three distinct substrate binding sites: one for nucleotide, one for ammonium ion and one for amino acids (see Section 3). However, an extensive search through the literature reveals that the inhibition of GS has largely focused on amino acid site ligands, a fact that holds true even for the natural inhibitors produced by a number of organisms. Methionine sulfoximine is one of the best known inhibitors of GS. It was originally isolated from nitrogen chloride-treated zein [106] as the toxin responsible for the induction of convulsions, hysteria and epileptic fits in a number of animals [107]. The mechanism of GS inactivation by MetSox has been discussed in Section 3. Phosphinothricin (a.k.a. glufosinate), pro-

duced as the tripeptide L-phosphinothricyl-L-alanyl-L-alanine (a.k.a. bialophos) by the bacterium *Streptomyces viridochromogene*, is similar in kinetic characteristics to MetSox. It has been modified extensively ([108] and others) to probe the characteristics of the GS binding site. Both the natural tripeptide and the single amino acid have been developed as herbicides. Yet another potent inhibitor found in nature is the antibiotic tabtoxinine-β-lactam, produced by *Pseudomonas* pv. *tabaci* [109].

Recently, Horwitz and associates have reported that the inhibition of GS secreted by *M. tuberculosis* is sufficient to halt the growth of the bacterium [110], suggesting that TB-GS might be a valid target for anti-tuberculosis drug-design. The structure of TB-GS is currently being solved to aid in the design of novel inhibitors for this enzyme [15]. In Table 3, we attempt to present a comprehensive list of the known synthetic inhibitors of GS, as well as their origin and species-dependent inhibition constants when available.

7. Conclusions

In the year 2000, the biochemical community has made good progress on understanding the structure, action, and regulation of bacterial GS Is. Our understanding of GS IIs from higher cells is still relatively primitive, with major questions about subunit structure, cofactors, and regulation still open.

Acknowledgements

We thank our previous coworkers for many stimulating discussions of GS, most particularly Elizabeth Goldsmith, Wolfgang and Helga Kabsch, Roger Fenna, Robert J. Almassy, Zachary Burton, Mary Lei, Ueli Aebi, Shwu-Huey Liaw, Gyo Jun, Frederic J. Wedler and Mason Yamashita. We thank the NIH for support. S.H.R. is a Howard Hughes Medical Institute Predoctoral Fellow.

References

[1] A. Ginsburg, Adv. Protein Chem. 26 (1972) 1–76.
[2] P.B. Chock, E.R. Stadtman, Methods Enzymol. 64 (1980) 297–325.
[3] E.R. Stadtman, A. Ginsburg, in: P.D. Boyer (Ed.), The Enzymes, Vol. 10, Academic Press, New York, 1974, pp. 755–807.
[4] F.C. Wedler, R. Toms, in: V.L. Schramm, F.C. Wedler (Eds.), Manganese in Metabolism and Enzyme Function, Academic Press, New York, 1986, pp. 221–238.
[5] D.L. Purich, in: D.L. Purich (Ed.), Amino Acid Metabolism Part A Vol. 72, John Wiley and Sons, 1998, pp. 9.
[6] R.J. Almassy, C.A. Janson, R. Hamlin, N. Xuong, D. Eisenberg, Nature 323 (1986) 304–309.
[7] M. Yamashita, R. Almassy, C. Janson, D. Cascio, D. Eisenberg, J. Biol. Chem. 264 (1989) 17681–17690.
[8] S.H. Liaw, C. Pan, D. Eisenberg, Proc. Natl. Acad. Sci. USA 90 (1993) 4996–5000.
[9] G.M.U. Pfluegl, H. Gill, D. Eisenberg, IUCR 24 (1996) C238.
[10] M. Pellegrini, N. Grønbech-Jensen, J.A. Kelly, G.M.U. Pfluegl, T.O. Yeates, Proteins 29 (1997) 426–432.
[11] H. Gill, G.M.U. Pfluegl, D. Eisenberg, Manuscript in preparation.
[12] S. Bancroft, S.G. Rhee, C. Neumann, S. Kustu, J. Bacteriol. 134 (1978) 1046–1055.
[13] Y. Chen, K. Backman, B. Magasanik, J. Bacteriol. 250 (1982) 214–220.
[14] F.R. Bloom, M.S. Levin, F. Foor, B. Tyler, J. Bacteriol. 134 (1978) 569–577.
[15] H. Gill, G.M.U. Pfluegl, D. Eisenberg, Acta Cryst. D 55 (1999) 865–868.
[16] R.C. Valentine, B.M. Shapiro, E.R. Stadtman, Biochemistry 7 (1968) 2143–2152.
[17] J. Hunt, P. Smyrniotis, A. Ginsburg, E. Stadtman, Arch. Biochem. Biophys. 166 (1975) 102–124.
[18] B.M. Shapiro, A. Ginsburg, Biochemistry 7 (1968) 2153–2167.
[19] J. Hunt, A. Ginsburg, J. Biol. Chem. 255 (1980) 590–594.
[20] M. Lei, U. Aebi, E.G. Heidner, D. Eisenberg, J. Biol. Chem. 254 (1979) 3129–3134.
[21] J. Moss, S.J. Stanley, R.L. Levine, J. Biol. Chem. 265 (1990) 21056–21060.
[22] B.M. Shapiro, E.R. Stadtman, J. Biol. Chem. 243 (1968) 3769–3771.
[23] R.L. Levine, L. Mosoni, B.S. Berlett, E.R. Stadtman, Proc. Natl. Acad. Sci. USA 93 (1996) 15036–15040.
[24] S.H. Liaw, J.J. Villafranca, D. Eisenberg, Biochemistry 32 (1993) 7999–8003.
[25] J. Vorhaben, L. Wong, J. Campbell, Biochem. J. 135 (1973) 893–896.
[26] P.R. Krishnaswamy, V. Pamijians, A. Meister, J. Biol. Chem. 235 (1960) PC39–PC40.
[27] P. Krishnaswamy, V. Pamiljans, A. Meister, J. Biol. Chem. 237 (1962) 2932–2940.
[28] C.F. Midelfort, I.A. Rose, J. Biol. Chem. 251 (1976) 5881–5887.
[29] T.D. Meek, J.J. Villafranca, Biochemistry 19 (1980) 5513–5519.

[30] A. Meister, in: Glutamine: Metabolism, Enzymology and Regulation, Academic Press, New York, 1980, pp. 1–40.
[31] S.H. Liaw, D. Eisenberg, Biochemistry 33 (1994) 675–681.
[32] A. Meister, in: P.D. Boyer, H. Lardy, K. Myrback (Eds.), The Enzymes, Vol. 6, 2nd edn., Academic Press, New York, 1962, pp. 443–469.
[33] J.M. Buchanan, S.C. Hartman, Adv. Enzymol. 21 (1959) 199–256.
[34] F.C. Wedler, P.D. Boyer, J. Biol. Chem. 247 (1972) 984–992.
[35] F.C. Wedler, B.R. Horn, J. Biol. Chem. 251 (1976) 7530–7538.
[36] J.R. Knowles, Annu. Rev. Biochem. 49 (1980) 877–919.
[37] J. Pace, E.E. McDermott, Nature 169 (1952) 415–416.
[38] R. Ronzio, A. Meister, Proc. Natl. Acad. Sci. USA 59 (1968) 164–170.
[39] C. Eads, R. LoBrutto, A. Kumar, J.J. Villafranca, Biochemistry 27 (1988) 165–170.
[40] J. Gass, A. Meister, Biochemistry 9 (1970) 1380–1390.
[41] R.E. Weisbrod, A. Meister, J. Biol. Chem. 248 (1973) 3997–4002.
[42] A. Shrake, E. Whitley, A. Ginsburg, J. Biol. Chem. 255 (1980) 581–589.
[43] A. Shrake, A. Ginsburg, J. Biol. Chem. 257 (1982) 8238–8342.
[44] S.H. Liaw, I. Kuo, D. Eisenberg, Protein Sci. 4 (1995) 2358–2365.
[45] M.R. Maurizi, A. Ginsburg, J. Biol. Chem. 257 (1982) 7246–7251.
[46] R. Haschemeyer, J. Wall, J. Hainfield, M. Maurizi, J. Biol. Chem. 257 (1982) 7252–7253.
[47] R. Timmons, S. Rhee, D. Luterman, P. Chock, Biochemistry 13 (1974) 4479–4485.
[48] R. Ronzio, W. Rowe, A. Meister, Biochemistry 8 (1969) 1066–1075.
[49] R. Weisbrod, A. Meister, J. Biol. Chem. 248 (1973) 3997–4002.
[50] S. Rhee, P. Chock, J. Biol. Chem. 256 (1981) 644–648.
[51] C.A. Woolfolk, E.R. Stadtman, Arch. Biochem. Biophys. 118 (1967) 736–755.
[52] H. Gill, G.M.U. Pfluegl, D. Eisenberg, Protein Sci. 5 (1996) 125.
[53] S.G. Rhee, J.J. Villafranca, P.B. Chock, E.R. Stadtman, Biochem. Biophys. Res. Commun. 78 (1977) 244–250.
[54] A. Ginsburg, Biochemistry 8 (1969) 1726–1740.
[55] P.D. Ross, A. Ginsburg, Biochemistry 8 (1969) 4690–4695.
[56] F.W. Dahlquist, D.L. Purich, Biochemistry 14 (1975) 1980–1989.
[57] S.H. Liaw, G. Jun, D. Eisenberg, Biochemistry 33 (1994) 11184–11188.
[58] M. Alibhai, J. Villafranca, Biochemistry 33 (1994) 682–686.
[59] A. Ginsburg, E. Gorman, S. Neece, B. Blackburn, Biochemistry 26 (1987) 5989–5996.
[60] Y. Kumada, D.R. Benson, D. Hillemann, T.J. Hosted, D.A. Rochefort, C.J. Thomson, W. Wohlleben, Y. Tateno, Proc. Natl. Acad. Sci. USA 90 (1993) 3009–3013.
[61] R.H. Haschemeyer, Trans. New York Acad. Sci. 30 (1968) 875–891.
[62] A. Meister, in: The Enzymes, P.D. Boyer (Ed.), Vol. 10, 3rd edn., Academic Press, New York, 1974, pp. 699–754.
[63] M. Carlsson, A. Carlsson, Trends Neurosci. 13 (1990) 272–276.
[64] A.B. Young, J.T. Greenamyre, Z. Hollingsworth, R. Albin, C. D'Amato, I. Shoulson, J.B. Penney, Science 241 (1988) 981–983.
[65] J. Hardy, R. Cowburn, Trends. Neurosci. 10 (1987) 406.
[66] M.D. Norenberg, J. Histochem. Cytochem. 27 (1979) 756–762.
[67] W.B. Rowe, R.A. Ronzio, V.P. Wellner, A. Meister, Methods Enzymol. 17 (1970) 900–911.
[68] T.F. Deuel, A. Lerner, D. Albrycht, Biochem. Biophys. Res. Commun. 48 (1972) 1419–1425.
[69] S. Tate, F. Leu, A. Meister, J. Biol. Chem. 247 (1972) 5312–5321.
[70] S. Tate, A. Meister, Proc. Natl. Acad. Sci. USA 68 (1971) 781–785.
[71] A. Meister, in: D. Haeussinger, R. Sies (Eds.), Glutamate Metabolism in Mammalian Tissues, Springer Verlag, Berlin, 1984, pp. 3–15,.
[72] J. Stahl, J. Jaenicke, Biochemistry 29 (1972) 401–407.
[73] J. Jaenicke, W. Berson, Hoppe Seyler's Z. Physiol. Chem. 358 (1977) 883–889.
[74] H.B. Pinkofsky, M.R. Maurizi, A. Ginsburg, Fed. Proc. Fed. Am. Soc. Exp. Biol. 44 (1985) 1807.
[75] M.R. Maurizi, H.B. Pinkofsky, P.J. McFarland, A. Ginsburg, Arch. Biochem. Biophys. 246 (1986) 494–500.
[76] M.R. Maurizi, H.B. Pinkofsky, A. Ginsburg, Biochemistry 11 (1987) 5023–5031.
[77] H. Yamamoto, H. Konno, T. Yamamoto, K. Ito, M. Mizugaki, Y. Iwasaki, J. Neurochem. 49 (1987) 603–609.
[78] A. Derouiche, T.G. Ohm, Neurosci. Lett. 165 (1994) 179–182.
[79] H. Tumani, G.Q. Shen, J.B. Peter, J. Immunol. Methods 188 (1995) 155–163.
[80] W.H. Elliot, Biochem. J. 49 (1951) 106–112.
[81] V.R.K.P. Pamiljans, G. Dumville, A. Meister, Biochemistry 1 (1962) 153–158.
[82] C. Monder, Biochemistry 4 (1965) 2677–2686.
[83] S. Wilk, A. Meister, R.H. Haschemeyer, Biochemistry 8 (1969) 3168–3174.
[84] R.A. Ronzio, W.B. Rowe, S. Wilk, A. Meister, Biochemistry 8 (1969) 2670–2674.
[85] F.C. Wedler, R.B. Denman, W.G. Roby, Biochemistry 24 (1982) 6389–6396.
[86] R.B. Denman, F.C. Wedler, Arch. Biochem. Biophys. 232 (1984) 427–440.
[87] F.C. Wedler, M.C. Vichnin, B.W. Ley, G. Tholey, M. Ledig, J.C. Copin, Neurochem. Res. 19 (1994) 145–151.
[88] F.C. Wedler, R.B. Denman, Curr. Top. Cell. Regul. 24 (1984) 153–169.
[89] S. Berl, D.D. Clark, in: L. Hertz, E. Kvamme, E.G. McGeer, A. Schousboe (Eds.), Glutamine, Glutamate, and GABA in the Central Nervous System: Proceedings of a Satellite Symposium of the 9th Meeting of the International Society for Neurochemistry on the Metabolic Relationship

between Glutamine, Glutamate, and GABA in the Central Nervous System, held in Saskatoon, Saskatchewan, Canada. A.R. Liss, New York, 1983, pp. 205–217,
[90] A.J.L. Cooper, F. Vergara, T.E. Duffy, in: L. Hertz, E. Kvamme, E.G. McGeer, A. Schousboe, (Eds.), Glutamine, Glutamate, and GABA in the Central Nervous System: Proceedings of a Satellite Symposium of the 9th Meeting of the International Society for Neurochemistry on the Metabolic Relationship between Glutamine, Glutamate, and GABA in the Central Nervous System, held in Saskatoon, Saskatchewan, Canada. A.R. Liss, New York, 1983, pp. 241–247.
[91] S.V. Tingey, F.Y. Tsai, J.W. Edwards, E.L. Walker, G.M. Coruzzi, J. Biol. Chem. 263 (1988) 9651–9657.
[92] F.C. Wedler, R. Toms, Fed. Proc. Fed. Am. Soc. Exp. Biol. 45 (1986) 1650.
[93] F.C. Wedler, B.W. Ley, Neurochem. Res. 19 (1994) 139–144.
[94] J. Moss, P.A. Watkins, S.J. Stanley, M.R. Purnell, W.R. Kidwell, J. Biol. Chem. 259 (1984) 5100–5104.
[95] W. Rowe, R. Ronzio, A. Meister, Biochemistry 8 (1969) 2674–2680.
[96] E. Layne, Methods Enzymol. 3 (1957) 447–454.
[97] M. Bradford, Anal. Biochem. 72 (1976) 248–254.
[98] J. Babul, E. Stellwagen, Anal. Biochem. 28 (1969) 216–221.
[99] A.V. Pushkin, L.P. Antoniuk, N.A. Solovieva, V.V. Shubin, Z.G. Evstigneeva, W.L. Kretovich, T.V. Cheednikova, V.L. Tsuprun, O.N. Zograf, N.A. Kiselev, Biochim. Biophys. Acta 828 (1985) 336–350.
[100] J.F. Mill, K.M. Mearow, H.J. Purohit, H. Haleem-Smith, R. King, E. Freese, Brain Res. Mol. Brain Res. 9 (1991) 197–207.
[101] R.W. Johnstone, B.E. Loveland, EMBL/GenBank/DDBY databases; http://www.expasy.ch/cgi-bin/niceprot.pl?P46410 (1994).
[102] J.E. Gouaux, O. Braha, M.R. Hobaugh, L. Song, S. Cheley, C. Shustak, H. Bayley, Proc. Natl. Acad. Sci. USA 91 (1994) 12828–12831.
[103] G.M.U. Pfluegl, D. Eisenberg, Protein Sci. 4 (1995) 125.
[104] J. Monod, J. Wyman, J.P. Changeux, J. Mol. Biol. 12 (1965) 88–118.
[105] M.R. Maurizi, A. Ginsburg, J. Biol. Chem. 257 (1982) 4271–4278.
[106] H. Bentley, E. McDermott, J.J.K.W. Pace, T. Moran, Nature 164 (1949) 438–439.
[107] P.J. Lea, S.M. Ridley, Soc. Exp. Biol. Semin. Ser. 38 (1989) 137–170.
[108] B. Lejczak, H. Starzemska, P. Mastalerz, Experientia 37 (1981) 461–462.
[109] P.L. Langston-Unkefer, P.A. Macy, R.D. Durbin, Plant Physiol. 76 (1984) 71–74.
[110] G. Harth, M. Horwitz, J. Exp. Med 189 (1999) 1425–1435.
[111] L.M. Abell, J.J. Villafranca, Biochemistry 30 (1991) 1413–1418.
[112] C.A. Woolfolk, B. Shapiro, E.R. Stadtman, Arch. Biochem. Biophys. 116 (1966) 177–192.
[113] C. Listrom, H. Morizono, B. Rajagopal, M. Mccann, M. Tuchman, N. Allewell, Biochem. J. 328 (1997) 159–163.
[114] M.A. Acaster, P.D.J. Weitzman, FEBS Lett. 189 (1985) 241–244.
[115] T. Meek, K. Johnson, J. Villafranca, Biochemistry 21 (1982) 2158–2167.
[116] J. Colanduoni, R. Nissan, J.J. Villafranca, J. Biol. Chem. 262 (1987) 3027–3043.
[117] L.M. Abell, J. Schineller, P.J. Keck, J.J. Villafranca, Biochemistry 34 (1995) 16695–16702.
[118] E.W. Logusch, D.M. Walker, J.F. McDonald, J.E. Franz, Biochemistry 28 (1989) 3043–3051.
[119] E.W. Logusch, D.M. Walker, J.F. McDonald, J.E. Franz, J.J. Villafranca, C.L. DiIanni, J.A. Colanduoni, B. Li, J.B. Schineller, Biochemistry 29 (1990) 366–372.
[120] M. Leason, D. Cunliffe, D. Parkin, P.J. Lea, B.J. Miflin, Phytochemistry 21 (1982) 855–857.
[121] E. Bayer, K.H. Gugel, K. Hägele, H. Hagenmaier, S. Jessipow, W.A. König, H. Zähner, Helv. Chim. Acta 55 (1972) 224–239.
[122] E.W. Logusch, D.M. Walker, J.F. McDonald, G.C. Leo, J.E. Franz, J. Org. Chem. 53 (1988) 4069–4074.
[123] D.M. Walker, J.F. McDonald, E.W. Logusch, J. Chem. Soc., Chem. Commun. (1987) 1710–1711.
[124] C.R. Johnson, B.R. Boettcher, R.E. Cherpeck, M.G. Dolson, Bioorg. Chem. 18 (1990) 154–159.
[125] E.W. Logusch, D.M. Walker, J.F. McDonald, J.E. Franz, Plant Physiol. 95 (1991) 1057–1062.
[126] O.W. Griffith, A. Meister, J. Biol. Chem. 253 (1978) 2333–2338.
[127] O.W. Griffith, M.E. Anderson, A. Meister, J. Biol. Chem. 254 (1979) 1205–1210.
[128] D.M. Walker, J.F. McDonald, J.E. Franz, E.W. Logusch, J. Chem. Soc. Perkin Trans. 1 (1990) 659–666.
[129] E.W. Logusch, Tetrahedron Lett. 29 (1988) 6055–6058.
[130] F.C. Wedler, B.R. Horn, W.G. Roby, Arch. Biochem. Biophys. 202 (1980) 482–490.
[131] N.A. Firsova, K.M. Selivanova, L.V. Alekseeva, Z.G. Evstigneeva, Biokhimiya 51 (1986) 850–855.
[132] G.K. Farrington, A. Kumar, F.C. Wedler, J. Med. Chem. 30 (1987) 2062–2067.
[133] S.J. Anandaraj, H.N. Jayaram, D.A. Cooney, A.K. Tyagi, N. Han, J.H. Thomas, M. Chitnis, J.A. Montgomery, Biochem. Pharmacol. 29 (1980) 227–245.
[134] S. Omura, M. Murata, N. Imamura, Y. Iwai, H. Tanaka, A. Furusaki, T. Matsumoto, J. Antibiot. 37 (1984) 1324–1332.
[135] M. Garcia-Dominguez, J. Reyes, F. Florencio, Proc. Natl. Acad. Sci. USA 96 (1999) 7161–7166.
[136] F. Gallardo, F.M. Canovas, Phytochemistry 31 (1992) 2267–2271.
[137] S. Fushiya, K. Maeda, T. Funayama, S. Nozoe, J. Med. Chem. 31 (1988) 480–483.
[138] N. Lustig, G. Mor, N. Lichtenstein, Isr. J. Chem. 9 (1971) 251–258.
[139] N. Lustig, H. Spiegelstein-Klarfeld, E. Schneider, N. Lichtenstein, Isr. J. Chem. 12 (1974) 757–763.
[140] M. Rabinovitz, M. Olson, D. Greenberg, Cancer Res. 17 (1957) 885–889.